Supplementary Material

Potassium Carbonate-based Ternary Transition Temperature Mixture (Deep Eutectic Analogues) for CO_2 Absorption: Characterizations and DFT Analysis

Hosein Ghaedi [a], Payam Kalhor [b], Ming Zhao [a,*], Peter T. Clough [c], Edward J. Anthony [c], Paul S. Fennell [d]

[a] School of Environment, Tsinghua University, Beijing 100084, China

[b] Department of Chemistry, Tsinghua University, Beijing 100084, China

[c] Energy and Power Theme, Cranfield University, Cranfield, Bedfordshire MK43 0AL, UK

[d] Department of Chemical Engineering, Imperial College London, South Kensington, London, SW7 2AZ, UK

[*]Corresponding author. Email: ming.zhao@tsinghua.edu.cn; Tel/Fax: +861062784701

Appendix A

1. CO_2 solubility measurement:

A set of equations was used to calculate the amount of CO_2 absorbed in the liquid samples. The total moles of CO_2 (n_{CO_2}) transferred from the mixing vessel (MV) to the equilibrium cell (EC) were determined according to the following equation:

$$n_{CO_2} = \frac{V_{MV}}{R \times T_{MV}} \left[\frac{P_1}{Z_1} - \frac{P_2}{Z_2} \right] \tag{S1}$$

where V_{MV} is the volume of MV; T_{MV} is the temperature of MV in K; R is the universal gas constant; P_1 is the initial pressure of MV before transferring CO_2 gas to EC and P_2 is the final pressure of mixing vessel after transferring gas when temperature stabilizes to initial temperature T; Z_1 and Z_2 are the compressibility factors for P_1 and P_2 of MV before and after transferring CO_2 at a constant temperature, respectively. In this research work, the Peng Robinson (PR) equation of state (EOS) has been used for the calculation of Z.

To calculate the equilibrium pressure ($P^{E}_{CO_2}$), the following equation was applied:

$$P^{E}_{CO_2} = P_{total} - P_v \tag{S2}$$

where P_{total} is the total pressure of the EC and P_v is the vapor pressure of TTM. Because of the low vapor pressure of TTMs and TTTMs, their P_v is negligible; thus, Eq. (S2) is modified to $P^{E}_{CO_2} \cong P_{total}$.

The remaining or unabsorbed moles of CO_2 ($n^{g}_{CO_2}$) in the gas phase were obtained from the following equation:

$$n^{\mathrm{g}}_{\mathrm{CO_2}} = \frac{V_{\mathrm{g}} \times P^{\mathrm{E}}_{\mathrm{CO_2}}}{Z \times R \times T_{\mathrm{EC}}} \tag{S3}$$

where V_g is the gas-phase volume of the EC; and Z and T_{EC} represent the compressibility factor and temperature of EC at the equilibrium point, respectively.

By applying Eq. (S4), the total moles of CO_2 dissolved in the liquid phase ($n^{l}_{CO_2}$) were determined:

$$n^{\mathrm{l}}_{\mathrm{CO_2}} = n_{\mathrm{CO_2}} - n^{\mathrm{g}}_{\mathrm{CO_2}} \tag{S4}$$

The final CO_2 solubility in TTMs was calculated according to the following equations:

In terms of mole fraction of CO_2 (x_{CO_2}),

$$x_{\mathrm{CO_2}} = \frac{n^{\mathrm{l}}_{\mathrm{CO_2}}}{n^{\mathrm{l}}_{\mathrm{TTM}} + n^{\mathrm{l}}_{\mathrm{CO_2}}} \tag{S5}$$

In terms of CO_2 loading (a_{CO_2}),

$$a_{\mathrm{CO_2}} = \frac{n_{\mathrm{CO_2}} - n^{\mathrm{g}}_{\mathrm{CO_2}}}{n^{\mathrm{l}}_{\mathrm{TTM/TTTM}}} \tag{S6}$$

where $n^{l}_{TTM/TTTM}$ is the moles of TTM or TTTM in the liquid phase which is determined from Eq. (S7)

$$n^{\mathrm{l}}_{\mathrm{TTM/TTTM}} = \left(\frac{\rho \times m \times V}{M} \right)_{\mathrm{TTM/TTTM}} \tag{S7}$$

where ρ and m are the density and mass fraction of TTM/TTTM, respectively; V is the volume of TTM or TTTM used for absorption and M is the molecular weight of TTM/TTTM.

2. FTI-R analysis

The C-C and C-NH_2 vibrational modes

The bands detected in the 1300 - 1100 cm^{-1} region are associated with the C-C and C-NH_2 stretching vibrations (Pavia et al., 2009). In pure AMPD, the bands at 1175.37 cm^{-1} and 1203.01 cm^{-1} are assigned to the C-NH_2 stretching and C-C stretching absorptions. But the peak of C-NH_2 stretching vibrations in TTTM did not appear and may be overlapped by the C-C stretching vibrations in the region of 1300 cm^{-1} to 1200 cm^{-1}.

The carbonate ion (CO_3^{2-}) vibrational mode

Another main functional group that is worthy of discussion here is carbonate ion (CO_3^{2-}). Regarding K_2CO_3 (see Fig. S3), two peaks at wavenumbers of 1446.29 cm^{-1} and 1358.41 cm^{-1} involve CO_3^{2-} out-of-plane antisymmetric stretching. A low-intensity peak at 1060.39 cm^{-1} represents CO_3^{2-} in-plane symmetric stretching. A peak at a wavenumber of 879.01 cm^{-1} is derived from the CO_3^{2-} out-of-plane antisymmetric bending mode. CO_3^{2-} in-plane symmetric bending vibrations occurred at wavenumbers of 817.07 cm^{-1} and 705.07 cm^{-1}. Other peaks in the spectra of potassium carbonate are a combination of these main peaks and called combination bands. A coupling of a fundamental vibration with an overtone or combination bands is called Fermi resonance. Normally, in components having a carbonyl group, Fermi resonance can be detected. Furthermore, the Fermi resonance intensities are usually greater than simple overtone band intensities (Larkin, 2011). A peak at 1749 cm^{-1} was an overtone of the CO_3^{2-} out-of-plane bending vibration at 879.01 cm^{-1} that is Fermi resonance enhanced with the carbonyl. A peak at 2994.27 cm^{-1} may be a combination of peaks with the wavenumbers of 1060.39 cm^{-1} and 879.01 cm^{-1} or a double of the peak at 1446.29 cm^{-1}. The

last peak at 3152.74 cm^{-1} might be a triple of the peak with the wavenumber of 1060.39 cm^{-1}. From Figs. 1 and 2, there is a peak at about 1300 cm^{-1} in both TTM and TTTM. These peaks which were at 1333.94 cm^{-1} in TTM and 1336.96 cm^{-1} in TTTM involve the CO_3^{2-} stretching bands in these components.

The C-OH vibrational mode

The wavenumbers between about 1100 cm^{-1} and 1030 cm^{-1} indicate the C-O stretching of species (Song et al., 2013). For pure AMPD, this stretching band had a wavenumber of 1041.41 cm^{-1}. For pure EG, this vibration was accompanied by two peaks at 1082.64 cm^{-1} and 1031.42 cm^{-1}. Besides, the C-O stretching vibrations were similar in intensity and wavenumber for the synthesized components (see Figs. 2 and 3). In the case of TTM, these vibrations appeared around 1084.90 cm^{-1} and 1039.94 cm^{-1}. Also for TTTM, C-O stretching appeared at the wavenumbers of 1085.39 cm^{-1} and 1039.11 cm^{-1}.

Here, bending vibrations in all components had a wavenumber between 1500-1100 cm^{-1}. The CH_2 scissoring at 1500 cm^{-1} and 1480 cm^{-1}, the CH_2 wagging at 1350 cm^{-1} and 1300 cm^{-1}, the CH_2 twisting at 1300 cm^{-1} and 1200 cm^{-1} and CH_2 rocking at 700 cm^{-1} and 600 cm^{-1} occurred in the case of pure EG and AMPD (see Figs. S3 and S4). Sometimes these vibrations are accompanied by more than one peak. It is evident from Fig. S3 that peaks with the wavenumbers 2626.58 cm^{-1} and 2528.70 cm^{-1} may be attributed to the overtones of CH_2 bending vibrations. Regarding the CH_3 bending vibrations for AMPD and synthesized solvents, the region for the CH_3 wagging was between 1480 cm^{-1} and 1400 cm^{-1}. The peaks at the wavenumbers of 1400 cm^{-1} and 1350 cm^{-1} are ascribed to the CH_3 scissoring vibrations.

Although the CH_3 rocking vibration appeared in the vicinity of 996.78 cm^{-1} in pure AMPD, this vibration did not occur in TTM and TTTM.

There was a peak at about 1650 cm^{-1} in the spectra of the synthesized components. For TTM, this peak may be a combination of peaks with the wavenumbers of 769 cm^{-1} and 880.86 cm^{-1}, as shown in Fig. 2. In the case of TTTM, this peak may be a combination of peaks at 769.58 cm^{-1} and 881.17 cm^{-1}, as illustrated in Fig. 3.

According to Figs. 2 and 3, both TTM and TTTM have similar spectra, except in two peaks. As displayed in Fig. 3, there were two peaks at 1594.11 cm^{-1} and 769.58 cm^{-1} for TTTM which were not observed for TTM. These peaks are ascribed to NH_2 bending and NH_2 wagging in TTTM because of the existence of nitrogen atoms in the structure.

3. Viscosity correlation

The experimental viscosity data were fitted as a function of temperature using the following equations (Ghaedi et al., 2017):

Vogel-Fulcher-Tammann (VTF) equation:

$$\ln(\eta) = A + \frac{B}{T - C} \tag{S8}$$

Andrade equation:

$$\ln(\eta) = A + \frac{B}{T} + C.\ln(T) \tag{S9}$$

Waterton equation:

$$\log_{10}(\eta) = \log_{10}(\eta_0) + \frac{B}{T}\exp\left(\frac{C}{T}\right) \tag{S10}$$

Arrhenius equation:

$$\ln(\eta) = \frac{E_a}{R.T} + \ln(\eta_\infty) \quad \text{(S11)}$$

Seddon equation:

$$\ln(\eta) = A + \frac{E_a}{R.T} + \ln(\eta_\infty) \quad \text{(S12)}$$

Yaws equation:

$$\log_{10}(\eta) = A + \frac{B}{T} + C.T + D.(T)^2 \quad \text{(S13)}$$

In the above equations, η is the dynamic viscosity of DESs in mPa.s; T is the temperature in K; A, B, C, and D are fitting parameters; η_∞ is the viscosity at infinite temperature; R is the gas constant and E_a is the activation energy of the solvents in J.mol^{-1}. It should be mentioned that the fitting parameters and η_∞ in Eqs. (S8)-(S13) are not the same and their values differ in different equations.

Appendix B

Table S1. Experimental viscosity, η, of pure EG, TTM and TTTM at temperature ranging from T = (293.15 to 343.15) K and p = 0.1 MPa.

T/K	Pure EG	TTM	TTTM
293.15	20.641	171.98	257.17
298.15	16.835	126.07	184.93
303.15	13.639	94.941	135.69
308.15	11.223	72.863	101.87
313.15	9.4250	56.969	77.753
318.15	7.8650	45.271	60.426
323.15	6.9650	36.528	47.756
328.15	5.7450	29.941	37.239
333.15	5.0540	24.800	30.341

Table S2. Experimental and literature viscosity (η, mPa.s) data of the EG.

T/K	Experimental data	Literature data (Yang et al., 2003)	$\%AAD$ [a]
293.15	20.641	20.833	0.3358
303.15	13.639	13.646	
313.15	9.4250	9.4430	
323.15	6.9650	6.9920	
333.15	5.0540	5.0600	

[a] $\%AAD = \frac{100}{n} \times \sum_{i=1}^{i=n} \frac{\left|Y_{\exp} - Y_{\text{lit}}\right|}{Y_{\exp}}$, where $Y_{\exp}$ and Y_{lit} represent experimental and literature data, respectively; n represents the number of the data point. (Murshid et al., 2018a; Murshid et al., 2018b)

Table S3. Fitting parameters of several models studied here, *RMSE* and R^2 for the viscosity of TTM and TTTM.

Parameters	TTM	TTTM
	VTF equation	
A	-2.678	-4.642
B	951.9	1536
C	171.5	142.4
R^2	0.9999	0.999
$RMSE \times 10^3$	0.80	6.20
	Andrade equation	
A	-259.9	-199.9
$B \times 10^{-4}$	1.624	1.39
C	36.9	27.82
R^2	0.9999	0.9999
$RMSE \times 10^2$	0.22	0.68
	Waterton equation	
$\mathrm{Log}_{10}(\eta_0)$	-0.5517	-1.450
A	119.3	334.9
B	564	357.4
R^2	0.9999	0.9999
$RMSE \times 10^2$	0.04	0.28
	Arrhenius equation	
$E_a \times 10^{-4}$	3.920	4.331
$\mathrm{Ln}(\eta_\infty)$	-10.98	-12.26
R^2	0.9980	0.9990
RMSE	0.03135	0.02441
	Yaws equation	
A	1.062	1.223
B	0.5531	0.7587
C	0.02547	0.0275
$D \times 10^5$	-7.39	-8.07
R^2	0.9855	0.9887
RMSE	0.04	0.04
	Seddon equation	
A	281.6	238.5
$E_a \times 10^{-4}$	3.920	4.331
$\mathrm{Ln}(\eta_\infty)$	-292.6	-250.8
R^2	0.998	0.999
RMSE	0.034	0.026
	Empirical equation (Eq. (1))	
A_0	-16.75	-48.22
$A_1 \times 10^{-4}$	1.189	3.926
$A_2 \times 10^{-6}$	-4.08	-12.03
$A_3 \times 10^{-8}$	6.135	13.94
R^2	1	1
$RMSE \times 10^3$	0.9	6.4

Table S4. The calculated activation energy (E_a/J.mol^{-1}) data for TTM and TTTM.

T/K	TTM	TTTM
293.15	45488.32	48633.38
298.15	43447.26	46620.47
303.15	41568.78	44890.39
308.15	39840.40	43419.01
313.15	38250.73	42184.39
318.15	36789.37	41166.57
323.15	35446.76	40347.34
328.15	34214.18	39710.11
333.15	33083.61	39239.71

Appendix C

(a)

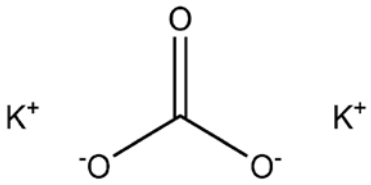

Potassium carbonate

(b)

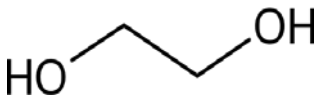

Ethylene glycol

(c)

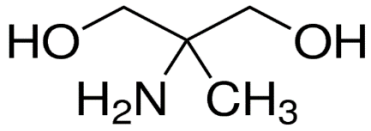

2-amino-2-methyl-1,3-propanediol

Fig. S1. Schematics of chemical structures of individual compounds.

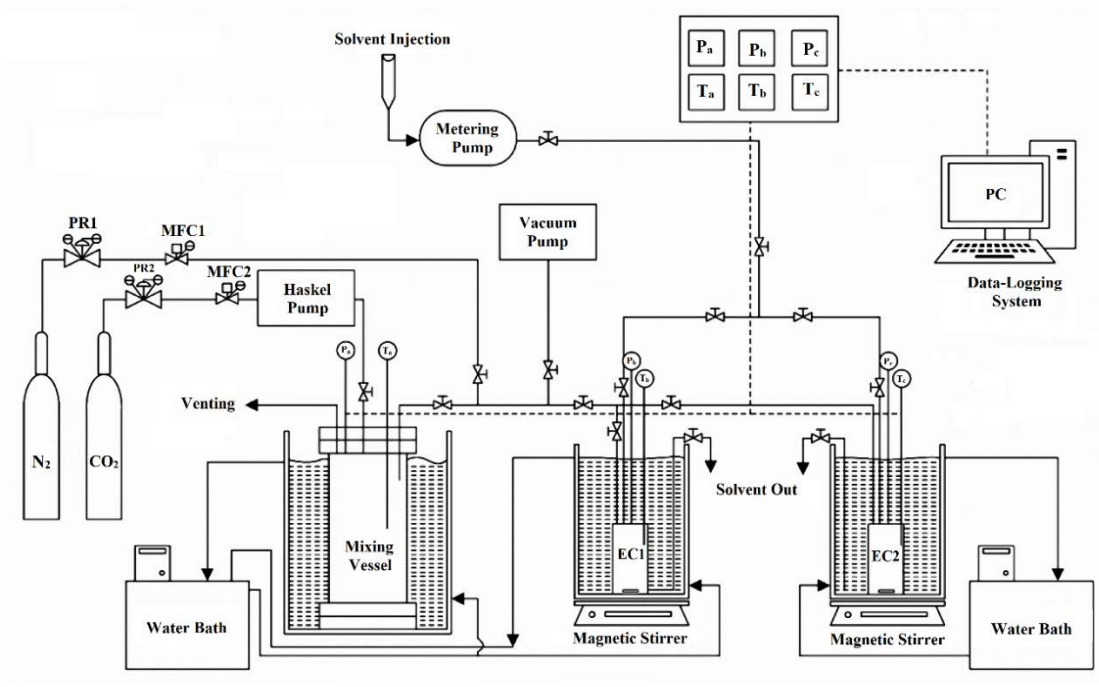

Fig. S2. Schematic of SOLTEQ BP-22 solubility cell used in this work.

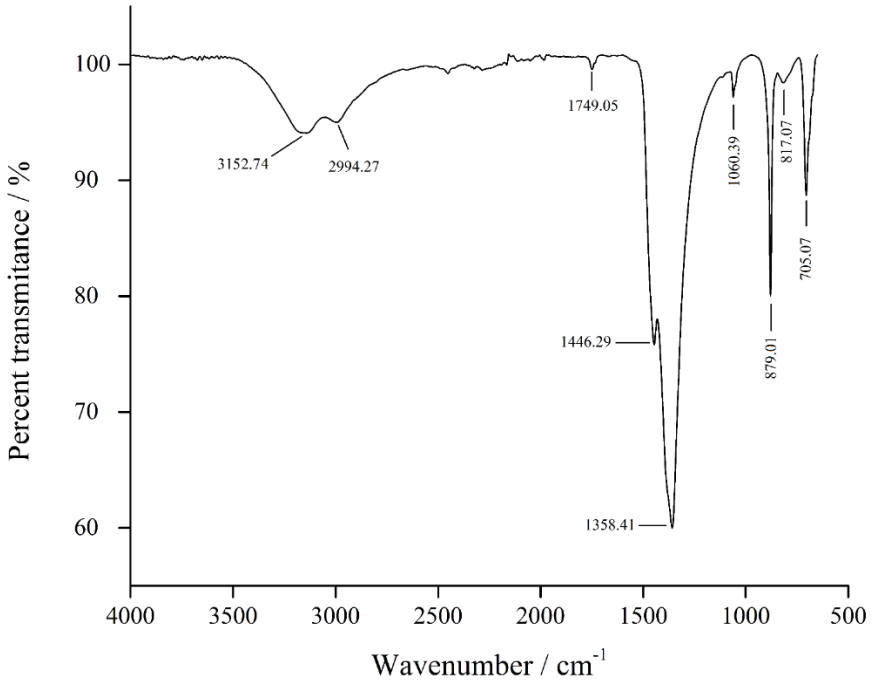

Fig. S3. Spectrum of K_2CO_3.

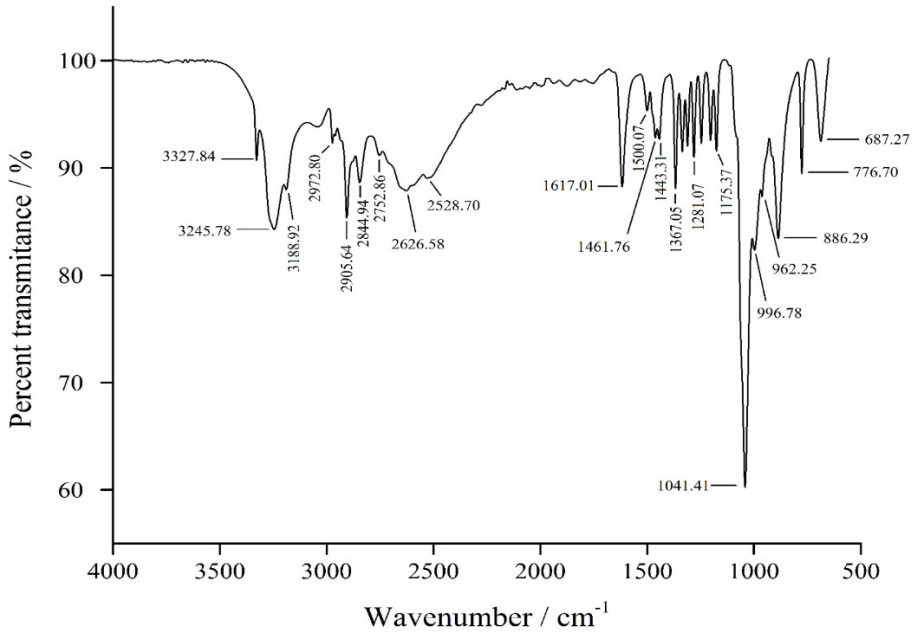

Fig. S4. Spectrum of AMPD.

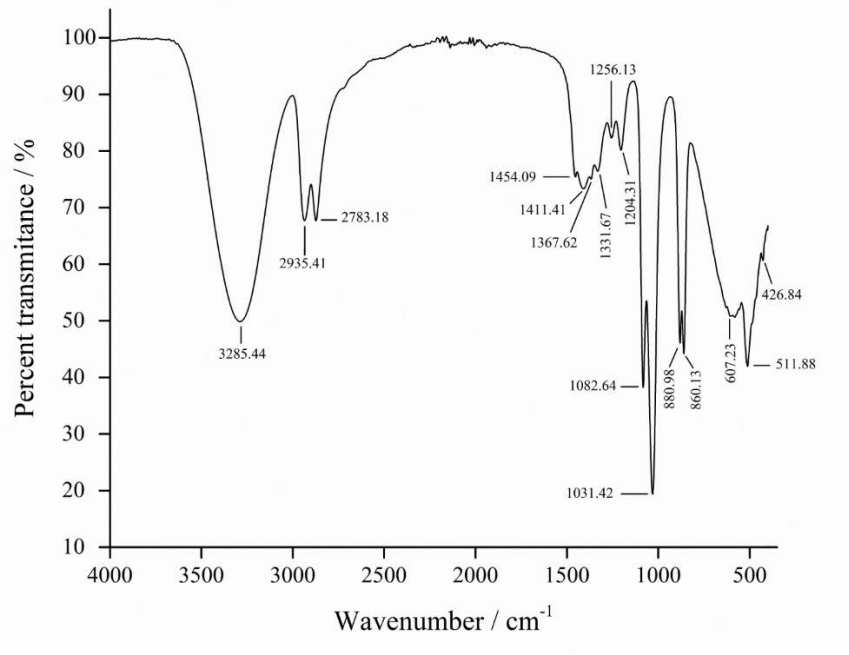

Fig. S5. Spectrum of EG.

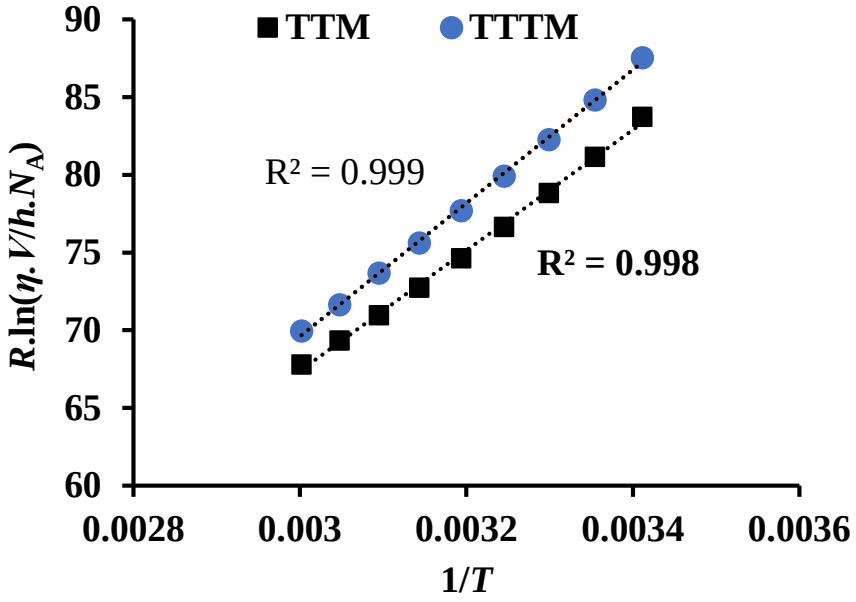

Fig. S6. Plots of $R.\ln(\eta.V/h.N_A)$ against $1/T$ for solvents.

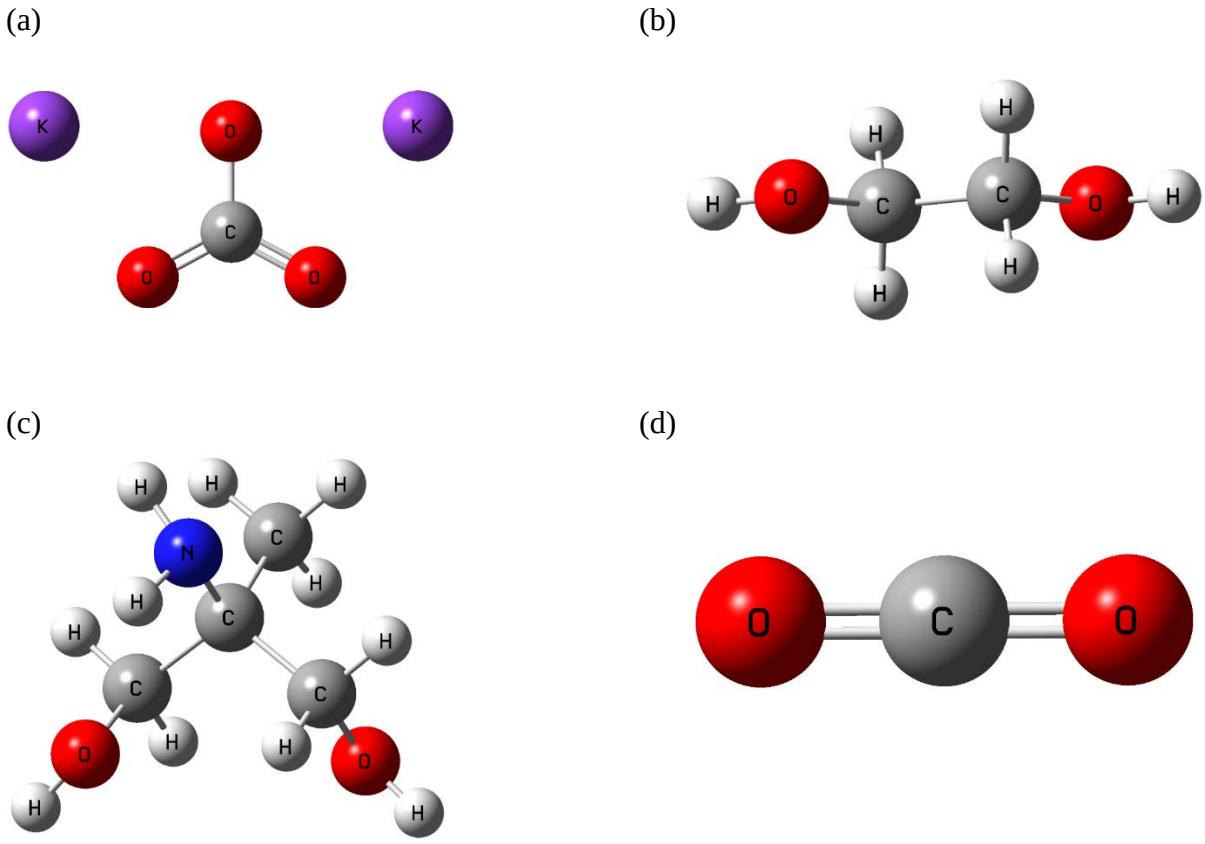

Fig. S7. The optimized structures of: (a) K_2CO_3, (b) EG, (c), AMPD, (d) free CO_2. Atom color code: (gray) carbon, (light gray) hydrogen, (red) oxygen, (purple) potassium, and (blue) nitrogen.

(a)

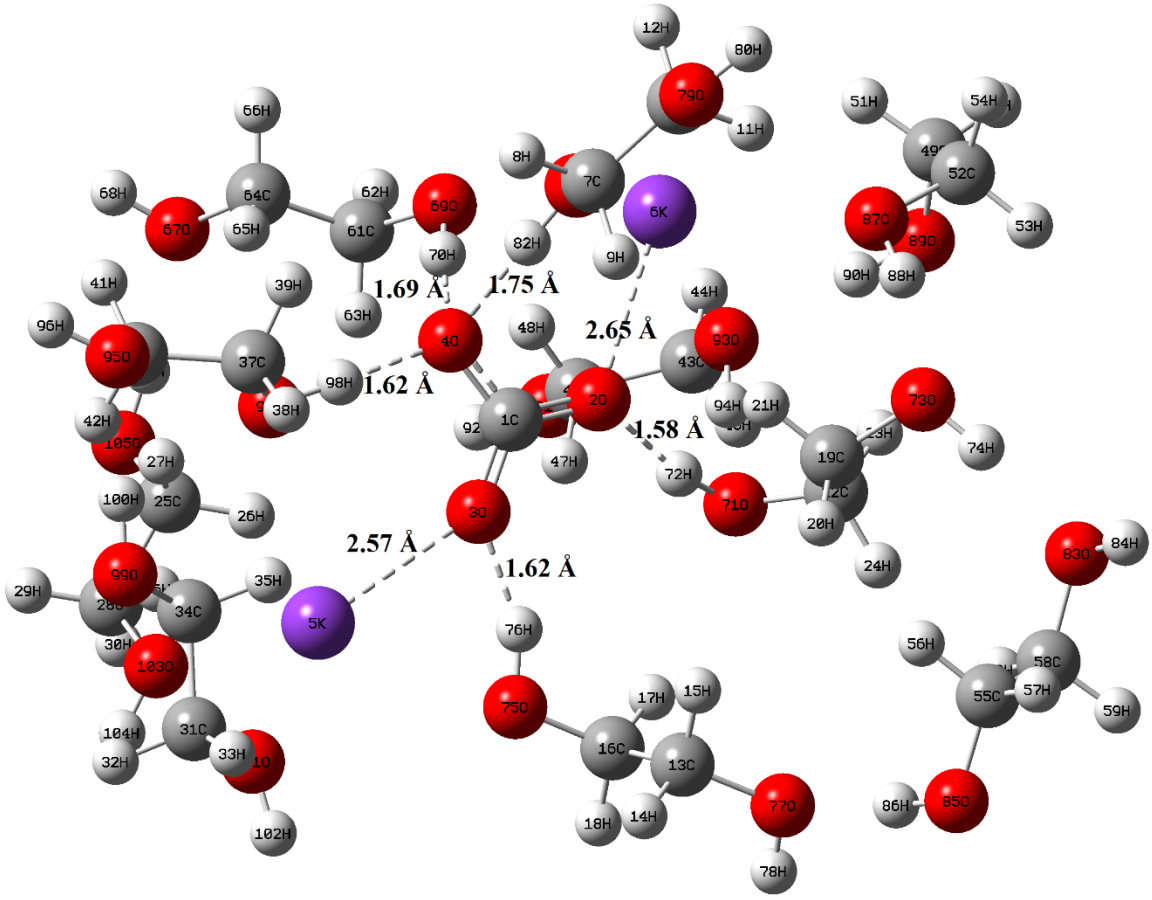

(b)

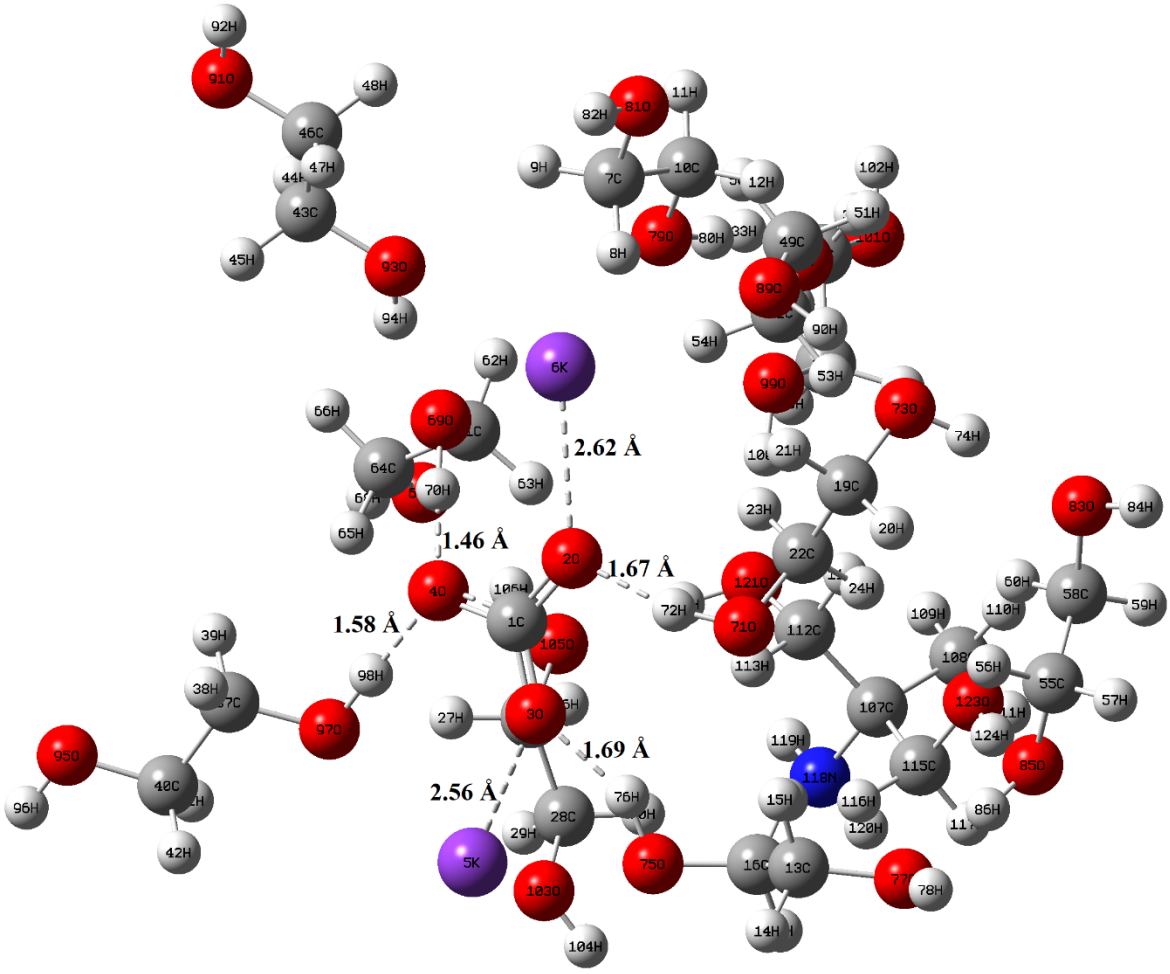

Fig. S8. The optimized structures of second geometries: (a) TTM (II) and (b) TTM (II). Atom color code: (gray) carbon, (light gray) hydrogen, (red) oxygen, (purple) potassium, and (blue) nitrogen.

References

Ghaedi, H., Ayoub, M., Sufian, S., Shariff, A.M., Lal, B., 2017. The study on temperature dependence of viscosity and surface tension of several Phosphonium-based deep eutectic solvents. J. Mol. Liq. 241, 500-510.
Larkin, P., 2011. Infrared and raman spectroscopy: principles and spectral interpretation. Elsevier, Waltham, USA.
Murshid, G., Ghaedi, H., Ayoub, M., Garg, S., Ahmad, W., 2018a. Experimental and correlation of viscosity and refractive index of non-aqueous system of diethanolamine (DEA) and dimethylformamide (DMF) for CO_2 capture. J. Mol. Liq. 250, 162–170.
Murshid, G., Ghaedi, H., Ayoub, M., Mjalli, F.S., Garg, S., 2018b. Volumetric properties of non-aqueous binary mixture of diethanolamine (DEA) and dimethylformamide (DMF). J. Env. Chem. Eng. 6, 6390-6398.
Pavia, D.L., Lampman, G.M., Kriz, G.S., Vyvyan, J.R., 2009. INTRODUCTION TO SPECTROSCOPY. Brooks/Cole, Cengage Learning, Washington, USA.
Song, W., Zhao, Z., Zheng, H., Wang, G., 2013. Gamma-irradiation synthesis of quaternary phosphonium cationic starch flocculants. Water Science and Technology 68, 1778.
Yang, C., Ma, P., Jing, F., Tang, D., 2003. Excess Molar Volumes, Viscosities, and Heat Capacities for the Mixtures of Ethylene Glycol + Water from 273.15 K to 353.15 K. Journal of Chemical & Engineering Data 48, 836-840.